Emission Mössbauer spectroscopy in TiO_2 single crystal

U. D. Wdowik* and K. Ruebenbauer
Mössbauer Spectroscopy Division, Pedagogical University, PL-30-084 Cracow, ulica Podchorążych 2, Poland
(Received 22 September 2000; revised manuscript received 13 November 2000; published 6 March 2001)

An almost perfect single crystal of TiO_2 was doped by about 50 ppm of ^{57}Co. Mössbauer spectra were measured versus sample orientation, temperature, and thermal history. It was found that Co occupies both substitutional and interstitial sites being a fast diffuser, while located interstitially. It decays to Fe^{3+} ($S=\frac{5}{2}$) in unperturbed lattice sites, Fe^{2+} ($S=2$) in lattice sites associated with the VO^{2-} vacancy, Fe^{2+} ($S=0$) in interstitial sites having adjacent VO^{2-}, and finally to Fe^{1+} ($S=\frac{3}{2}$) in unperturbed interstitial sites. Thermal history of the sample could be erased by heating to about 750 K. Substitutional iron following ^{57}Co decay could be observed solely in the host lattice at elevated temperatures. High-temperature data indicate two charge states of iron, i.e., Fe^{2+} and Fe^{3+}. Fe^{2+} with $S=2$ exists in the vicinity of defects and converts gradually to Fe^{2+} ($S=0$) with the increasing temperature, while Fe^{3+} ($S=\frac{5}{2}$) resides in the unperturbed lattice sites. A host matrix becomes more covalent at very high temperatures as well as slightly anharmonic. No significant diffusivity of the substitutional iron could be seen. The total area under the spectrum follows unusual pattern due to the gradual disappearance of the signal coming from iron located interstitially, i.e., a transfer of iron atoms into fast diffusing interstitials with increasing temperature occurs. All processes were observed to be reversible upon heating/cooling.

DOI: 10.1103/PhysRevB.63.125101 PACS number(s): 76.80.+y, 61.72.Ss, 61.72.Hh, 61.72.Cc

I. INTRODUCTION

Rutile (TiO_2) has been a subject of many different types of investigations, reviews of which are given by Millot *et al.*[1] This compound is frequently classified as an oxygen-deficient (metal-excess) nonstoichiometric oxide. The extent of the nonstoichiometry and the types of major defects in rutile are still a matter of discussion and a source of controversy as well. The nature of defects has been the subject of numerous studies with different techniques (see Ref. 1 and references therein for details). Generally, the studies indicate that titanium dioxide is oxygen deficient and suggest existence of predominant atomic point defects being either interstitial titanium ions or oxygen vacancies, or both, or combinations of these defects with impurities in the lattice.[2–6]

Rutile belongs to $P4_2/mnm$ space group. The crystal structure of rutile is schematically shown in Fig. 1. The cation sublattice constituted of titanium ions is body-centered tetragonal. Each titanium ion is surrounded by a slightly distorted octahedron of six oxygen ions. The octahedra are linked to each other forming chains parallel to the c axis. Between the chains are regions of low electron density, the so-called ''open channels'' or easy diffusion channels. At regular intervals of $c/4$ along the channel are potential minima which are possible interstitial sites for cations. The open channels cause anisotropy in the diffusion process and may allow fast diffusion of smaller ions parallel to the tetragonal axis.[5,6]

Features of the Mössbauer spectroscopy allow us to use it as a tool to study the behavior of dopants in the host lattice. A considerable fraction of investigations have focused on ^{57}Fe, with both stable iron and radioactive ^{57}Co as dopants. Although the behavior of iron as a dilute impurity is quite well understood now, however, much uncertainty about the relationship between the parent cobalt ion and the iron daughter ion which results from the ^{57}Co electron capture (EC) decay still exists. The resulting Mössbauer spectra of ^{57}Co-doped crystal may not relate to properties of the ideal crystal due to intrinsic crystal defects. It is also well known that very dilute dopants may lead to results quite different from those for percent dopants.[7,8]

Unfortunately, the Mössbauer spectroscopy cannot be done with absorbers containing iron in the ppm range. Therefore, to obtain ppm range spectra, rutile has to be doped with ^{57}Co, the latter decaying to ^{57}Fe. Such Mössbauer sources can give us some information about the behavior of iron in the ppm range. There are, however, some complications because the iron enters the lattice not directly, but rather as a cobalt ion, and the subsequent Auger processes frequently produce a number of different charge states of the resulting ions. It should be noted that the surrounding defect configu-

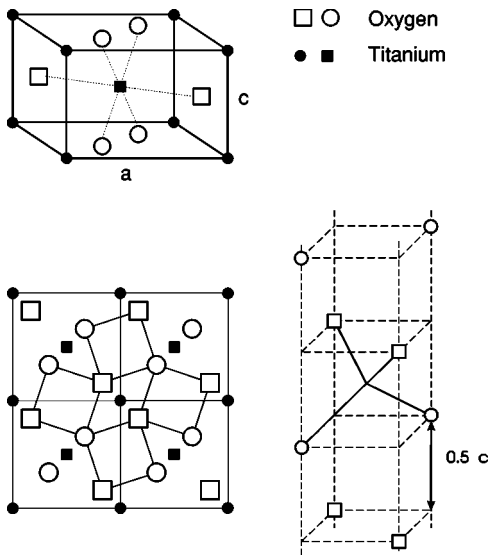

FIG. 1. Crystal structure of rutile and channel arrangement.

 ©2001 The American Physical Society

ration will be related still to the Co impurity and not to the Fe ion; at least during the lifetime of the excited ^{57}Fe Mössbauer state.

Impurity ions incorporated into the host matrix introduce uncompensated charge. Therefore the difference in the total charge of the crystal has to be compensated by introducing defects. Oxygen vacancies and interstitial ions are created to maintain charge neutrality.

In order to interpret the Mössbauer data of ^{57}Co doped rutile it seems reasonable to assume atomic point defect model based on simultaneous existence of interstitial Ti^{4+} and VO^{2-} vacancies. The virtual reaction of the formation of Ti^{4+} under the equilibrium conditions for pure rutile can be expressed as[5]

$$\mathrm{Ti}+2\mathrm{O}\rightleftharpoons \mathrm{Ti}^{4+}+4e+\mathrm{O}_2(g), \tag{1}$$

where Ti^{4+}, O, e denote cation, atom, and electron, respectively. The formation of oxygen vacancy under the equilibrium conditions is as follows:

$$\mathrm{O}\rightleftharpoons \mathrm{VO}^{2-}+2e+\frac{1}{2}\mathrm{O}_2(g). \tag{2}$$

The Mössbauer technique has been also applied to study diffusion processes in solids on the microscopic scale.[9] In most cases, the diffusivity measurements on TiO_2 have been performed with the radioactive-tracer sectioning technique.[5,6] A tracer impurity diffusion measurements suggest that both crystal and the point defect structures strongly influence the diffusivity in rutile.[5] The diffusion coefficients in TiO_2 are sensitive to electric charge of the impurity ions and exhibit a very strong anisotropy.[5,6] This large anisotropy is due to the open channels being parallel to the c axis.[5,6] The experimental results indicate that divalent impurity ions like Co can diffuse rapidly along the rutile open channels by the interstitialcy mechanism, while trivalent or mixed-valence impurities as Fe prefer lattice substitutional positions.[5] The impurity charge state is more important than its size as far as diffusivity in titanium dioxide is concerned.

The present paper is concerned with the study of the charge states and environment of ^{57}Fe ions in TiO_2 single crystal following ^{57}Co decay by using the Mössbauer effect as a microscopic probe to measure the internal crystalline fields and electronic charge densities at the ^{57}Fe nuclei. Additionally, the paper discusses results of the high-temperature Mössbauer measurements performed on TiO_2 single crystal doped with ^{57}Co.

The main aim of this work was to study the behavior of the very diluted dopant in single crystal of rutile at room and elevated temperatures. High temperature Mössbauer data obtained by means of the emission spectroscopy in TiO_2 single crystals is reported.

II. SOURCE PREPARATION

High-purity (completely transparent) and almost stoichiometric single crystal of TiO_2 was made by MaTeck. A plate having thickness of about 100 μm was cut with $\langle 111\rangle$ direction perpendicular to the surface of dimensions 4.3 $\times$5.6 mm. Neither rocking curve measurements nor standard diffraction patterns of the above plate detected measurable mosaicity.

A Mössbauer source was made by diffusing in 5 mCi of carrier-free ^{57}Co leading to about 50-at. ppm of Co and Fe resulting from decay altogether. Commercial 0.1-n aqueous solution of cobalt in HCl was diluted with deionized water and neutralized with the help of saturated ammonia vapor. Resulting solution was deposited on the crystal and dried. Subsequently the sample was slowly heated to 1173 K under the 20% O_2/80% He partial pressure mixture flow at normal pressure. The sample was kept in the Pt boat. The same kind of atmosphere and sample holder were used during the measurements.

A control sample was made in the same way with the natural cobalt. X-ray patterns and rocking curves are the same for the undoped crystal and the above control sample. Doped samples acquired pale yellow color distributed evenly within the sample volume.

III. EXPERIMENT

A. Sample environment

The sample in a holder described above was placed in a furnace equipped with the uniaxial goniometer which allowed to rotate the sample *in situ*. Mössbauer data were collected for a beam outgoing in the $[\bar{1}10]$ plane along the following directions: $\langle 110\rangle$, 12.2° from the $\langle 110\rangle$ axis, $\langle 111\rangle$, 37.5°, and 49.5° from the $\langle 110\rangle$ axis. A goniometer rotation axis was parallel to the largest dimension of the sample. The hot zone of the furnace employs solely high-purity alumina, platinum, rhodium, sample material, and protective atmosphere. A heater is separated from the sample area by the vacuum tight alumina tube. A temperature was controlled by means of Pt-Pt (10% Rh) thermocouple. The beam exit window having 22-mm diameter was made of iron-free beryllium. A distance between sample and the window was about 165 mm. The sample remained uncovered from the top. A computer based virtual temperature controller was used to maintain sample temperature within 2-K accuracy.

B. Data collection

A single line $K_4\,^{57}Fe(CN)_6\times 3H_2O$ vibrating absorber in conjunction with Kr-filled proportional detector was used to collect spectra. A typical γ-ray spectrum is shown in Fig. 2. One can notice x-ray fluorescent lines originating in the Pt sample holder mainly due to the 124-keV line. Normal and anticoincidence spectra were measured for each Mössbauer spectrum in order to evaluate background under the resonant line. A typical background measured as $\lambda=(S+B)/S$, where S stands for a contribution due to the 14.4-keV line, while B is a contribution due to other photons, was 1.1.

Mössbauer spectra were collected in a multiscaler round corner triangular mode in 4096 channels[10] and subsequently folded with addition of two adjacent channels. Spectra were measured at well defined elevated temperatures for sample orientations specified above and subsequently for the same

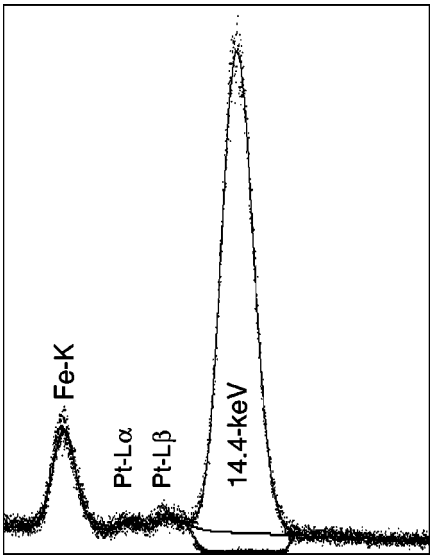

FIG. 2. Typical direct γ-ray spectrum with the overlaid anticoincidence spectrum showing single-channel analyzer window.

orientations having the sample quenched to room temperature. A temperature range covered extended from room temperature (RT) until 1388 K. The cooling curve of the furnace upon having switched off power is almost exponential with the time constant being about 19 min.

C. Data processing

Mössbauer spectra were fitted to multiple sites described by the hyperfine Hamiltonians assigned to each site. It was found that there is no directional dependence of the line intensities. A Lorentzian approximation was used as the source resonant thickness is negligible.[11] Typical values of χ^2 were ranging from 0.8 to 1.0, while MISFIT[12,13] ranged from 0.13% at low temperatures to 4.3% at the highest temperatures.

IV. RESULTS

Spectra measured at room temperature after quenching from elevated temperature depend solely upon the initial temperature. They do not depend upon the sample orientation.

A spectrum shape is perfectly reproducible after the same thermal history of the sample. A memory of the previous thermal history could be erased by heating the sample to about 750 K for 24 h. The activity remains inside the sample volume as the count rate decreases solely due to the radioactive decay of cobalt. Typical spectra of the quenched sample are shown in Fig. 3.

Each RT spectrum consists of the components listed in Table I. Hyperfine parameters of the above components are summarized in Table II. Linewidths of particular components and the total channel contribution are listed in Table III. A lattice contribution follows from the normalization to unity. Quadrupole splittings and shifts are independent of the initial temperature once the equilibrium at high temperature is reached, and the cooling rate is fast enough (no more than half an hour from the initial temperature to 750 K).

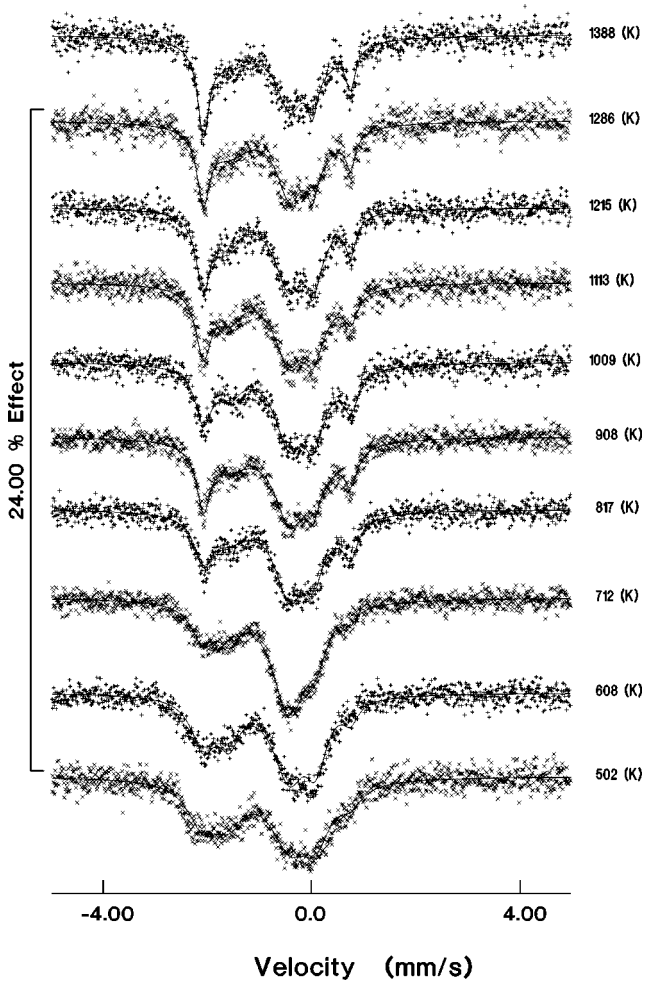

FIG. 3. Mössbauer spectra versus quench temperature for ⟨111⟩ sample orientation.

All results obtained below 750 K originate from the initially slowly cooled sample from 1173 K (10 h cooling time). The annealing sequence for these low temperatures as follows: 8 days at 502 K, 8 days at 402 K, 9 days at 608 K, and 9 days at 712 K.

Typical high-temperature spectra are shown in Fig. 4. No signal from interstitials could be observed at elevated temperatures. Remaining iron was found to be in two valence states, namely, Fe^{3+} and Fe^{2+} located at regular lattice positions. Divalent iron exists in two spin configurations, i.e., $S=2$ and $S=0$. Upon raising temperature high enough the high spin Fe^{2+} tends to convert to low spin Fe^{2+}. Hence a contribution corresponding to high spin Fe^{2+} decreases (see Table IV). This component disappears above approximately

TABLE I. Components of the room-temperature spectra.

No.	Valence	Charge and spin configuration	Location
1	Fe^{3+} $(S=\frac{5}{2})$	[Ar] $3d^5$ ↑ ↑ ↑ ↑ ↑	lattice
2	Fe^{2+} $(S=2)$	[Ar] $3d^6$ ↑↓ ↑ ↑ ↑ ↑	lattice
3	Fe^{2+} $(S=0)$	[Ar] $3d^6$ ↑↓ ↑↓ ↑↓	channel
4	Fe^{1+} $(S=\frac{3}{2})$	[Ar] $3d^7$ ↑↓ ↑↓ ↑ ↑ ↑	channel

TABLE II. Hyperfine parameters of the RT spectra. Δ denotes quadrupole splitting and I.S. stands for a total shift versus metallic iron. Positive velocity corresponds to source approaching absorber. One has to note that hyperfine structure is measured within the source.

No.	I.S. [mm/s]	Δ [mm/s]
1	−0.46(2)	0
2	−0.77(1)	1.72(4)
3	0.34(1)	0.73(2)
4	−2.12(1)	0

800 K. This effect is related to the increased covalency with temperature. Quadrupole splitting of Fe^{2+} with $S=2$ is temperature dependent as it is shown in Fig. 5. Population of $3d$ orbitals equilibrates with increasing temperature accounting for the observed decrease in quadrupole splitting.

Fe^{3+} ($S=\frac{5}{2}$) seems to be a quite stable iron valence state in a rutile lattice, since it was encountered in the whole temperature region studied. An apparent reduction to divalent iron may be seen above 1000 K (see Fig. 6). The solid lines in Fig. 6 represent the slope 7.31×10^{-4} mm/sK due to the Dulong-Petit rule.

The data included in Table IV indicate that no significant broadening of linewidths corresponding to substitutional impurities was detected, i.e., no lattice diffusion was observed. High-temperature spectra do not depend upon sample orientation as well as the spectra of the quenched sample.

V. DISCUSSION AND CONCLUSIONS

An impurity is able to enter the host TiO_2 lattice substitutionally and/or interstitially. Therefore multiple valence states of ^{57}Fe represent different and distinguishable local environments in which the impurities could reside in the host lattice. EC decay converts the parent $^{57}Co^{2+}$ located at the regular lattice positions either to Fe^{2+} or Fe^{3+} daughter ions. The oxidation state of the daughter ion depends on the impurity surrounding, i.e., it is mainly related to a variety of possible defects. Almost stoichiometric rutile is to some extent oxygen-deficient material and the tetravalent titanium interstitials are present as well.

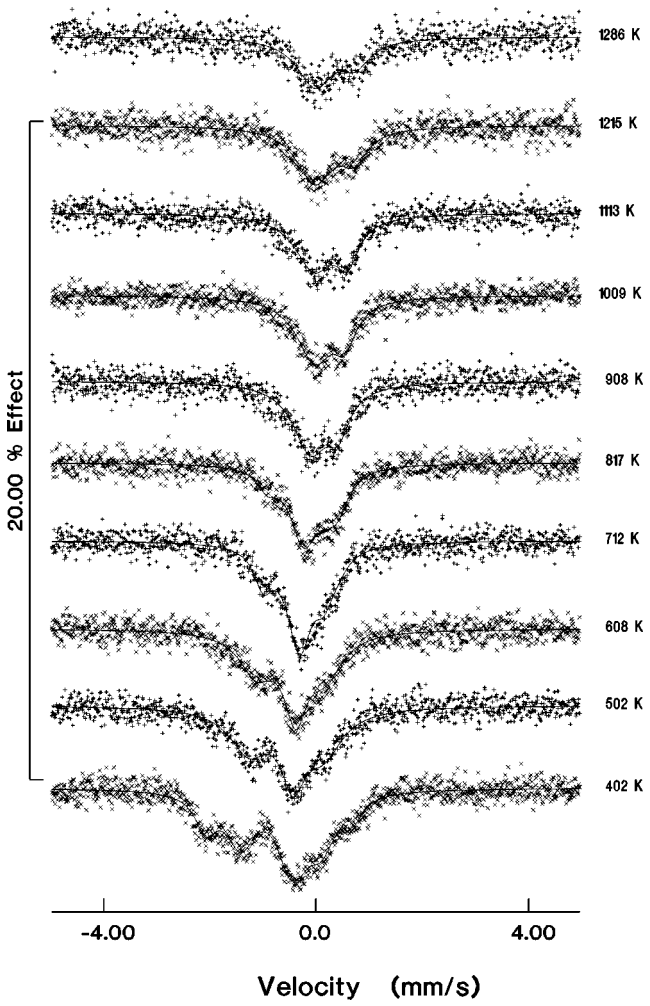

FIG. 4. Typical high-temperature spectra for ⟨111⟩ sample orientation.

Trivalent iron is a result of Co EC decay, provided the parent atom is isolated and located in undisturbed (at least locally ideal) substitutional cation site. In other words, the

TABLE III. Linewidths of particular components and the total channel contribution at room temperature. A temperature shown denotes the initial temperature of quench.

	Linewidth [mm/s]				
T[K]	Fe^{3+} ($S=5/2$)	Fe^{2+} ($S=2$)	Fe^{2+} ($S=0$)	Fe^{1+} ($S=3/2$)	Channel contribution [%]
502(1)	0.88(6)	0.69(7)	0.52(7)	0.73(5)	34(2)
608(1)	0.78(3)	0.47(4)	0.35(4)	0.57(3)	30(1)
712(2)	0.79(2)	0.46(4)	0.29(5)	0.55(4)	19(1)
817(4)	0.67(3)	0.90(9)	0.34(2)	0.42(4)	32(1)
908(1)	0.71(3)	0.92(7)	0.32(2)	0.32(2)	31(1)
1009(2)	0.68(3)	0.60(6)	0.38(2)	0.39(3)	37(1)
1113(1)	0.71(3)	0.63(5)	0.33(2)	0.34(2)	33(1)
1215(2)	0.69(4)	0.56(8)	0.25(3)	0.34(2)	35(1)
1286(2)	0.59(4)	0.95(8)	0.23(2)	0.29(2)	29(1)
1388(2)	0.61(5)	1.10(10)	0.23(2)	0.27(2)	32(1)

TABLE IV. Linewidths and contributions of particular components at elevated temperatures.

	Linewidth [mm/s]			Contributions [%]		
T[K]	Fe^{3+} ($S=5/2$)	Fe^{2+} ($S=2$)	Fe^{2+} ($S=0$)	Fe^{3+} ($S=5/2$)	Fe^{2+} ($S=2$)	Fe^{2+} ($S=0$)
402(1)	0.58(6)	0.69(6)		25(3)	50(4)	
502(1)	0.57(5)	0.90(5)		33(4)	67(4)	
608(1)	0.54(4)	0.81(5)		39(4)	61(4)	
712(2)	0.58(5)	0.44(5)	0.50(20)	59(6)	32(7)	9(3)
817(4)	0.64(9)	0.50(10)	0.55(7)	55(13)	20(15)	25(7)
908(1)	0.81(5)		0.54(7)	72(6)		28(6)
1009(2)	0.84(6)		0.51(7)	73(5)		27(5)
1113(1)	0.88(7)		0.53(7)	69(6)		31(6)
1215(2)	0.85(6)		0.60(1)	73(5)		27(5)
1286(2)	0.84(8)		0.70(1)	71(7)		29(7)

anion sublattice in the vicinity of impurity is complete. Two Fe^{3+} ions substitute for Ti^{4+} ion resulting in a single oxygen vacancy (VO^{2-}) maintaining charge neutrality. However, defects induced in the crystal are of nonlocal (extrinsic) character. Oxygen vacancies which accompany trivalent iron impurities are at the next-nearest-neighbor oxygen positions at least. Since Fe^{3+} do not feel the effect of far distant oxygen vacancies the spectral component due to trivalent iron was observed to remain practically unsplit. A quadrupole interaction is either very small or partly canceled, however, it influences the linewidth of this component. Moreover, Fe^{3+} does not exist as a channel residing impurity. It is generally accepted and also confirmed by diffusion studies[5,6] that ions with radii less than 0.73 Å (for example Fe^{3+}) cannot occupy channel sites of rutile.

Room-temperature spectra also show a presence of regular substitutional divalent iron for which the excited state, $I=\frac{3}{2}$, is split by a quadrupole interaction. The isomer shift and the quadrupole splitting are in the range characteristic for Fe^{2+} with spin configuration $S=2$ both. Co^{2+} residing at distorted oxygen octahedral surrounding, and being disturbed by the near-neighbor oxygen vacancy decays to a high spin Fe^{2+}. The broadened lines observed for this valence state suggest the existence of nonequivalent iron-vacancy complexes and possible slightly different cobalt-vacancy distances.

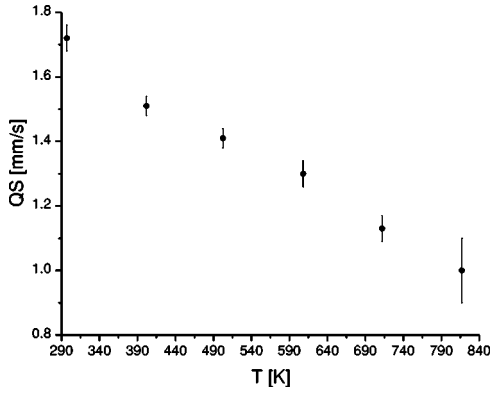

FIG. 5. Quadrupole splitting of Fe^{2+} ($S=2$) versus temperature.

The most interesting result is a presence of unusual Fe^{1+} ($S=\frac{3}{2}$) charge state. The resonance line corresponding to ''exotic'' monovalent iron was observed to have an isomer shift of -2.12 mm/s at RT. This very large shift indicates a charge state of $+1$ for the iron in a $3d^7$ configuration. The exotic iron is present solely after quench and at elevated temperatures not exceeding 400 K (see Fig. 7 for details). Monovalent iron is suggested to represent an isolated state. It is present only in a perfect, i.e., undisturbed tetrahedral channel surrounding. Therefore it produces a single resonance line of a large isomer shift, the latter indicating a very low electronic charge density at the iron nucleus. Fe^{1+} is a result of radioactive decay of parent cobalt ion diffusing rapidly along the open channels[5] and trapped into the ''ideal'' (free of intrinsic defects) interstitial potential minima by the abrupt quench. It should be noted, that Fe^{1+} represents a metastable state and it has been previously observed by emission Mössbauer spectroscopy,[14–18] the latter having the suitable time window of observation. It has been detected in single crystals being previously quenched and having the Co dopants in the ppm range diffused into.

For a Co impurity ''frozen'' in the channel disturbed by the oxygen vacancy at the neighborhood the daughter is Fe^{2+} with $S=0$. Hence this component represents some associated state, i.e., it is due to the existence of a local defect. One should note that this ion cannot be regarded as an ordinary substitutional one since its spectral component disappears at elevated temperatures (see Fig. 7).

It was observed that contributions corresponding to interstitials are practically temperature independent for the quench performed from initial temperatures exceeding approximately 750 K (see Table III for details). The appropriate thermal treatment is able to erase the previous thermal history of the sample. The data included in Table III indicate that in most cases a linewidth reduction in a channel is observed. The narrow lines suggest well-defined sites upon such an erasure.

The absence of a change in a doublet symmetry/asymmetry with the sample orientation relative to the direction of the γ-ray beam is due to multiple vacancy-impurity configurations. A lattice distortion in the vicinity of impurity averages to nearly cubic local symmetry over different sites,

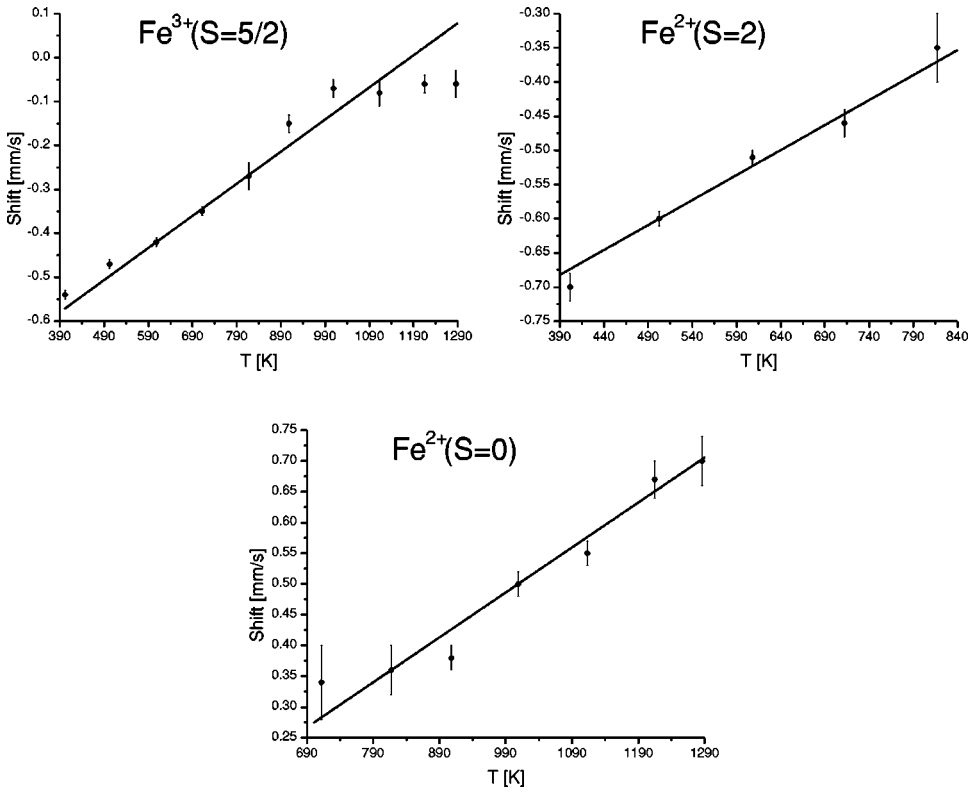

FIG. 6. Shifts of particular ^{57}Fe configurations versus temperature.

and hence accounts for the observed effect. Similar RT spectra were obtained by Nagy[19] and his co-workers upon independent diffusing ^{57}Co into a single crystal of TiO_2 from the same batch as ours.

The most remarkable result of the Mössbauer measurements performed at elevated temperatures is a disappearance of the signal coming from the channel at about 400 K. This is due to a very fast diffusivity of interstitial Co impurities and daughter Fe. The Mössbauer lines corresponding to dopants diffusing rapidly along the open channels via the interstitialcy/channel mechanism[5] become too broad to be detected[9] and give rise to the spectrum background. The strong evidence for such a behavior is the falloff in the temperature dependence of the spectrum total area (see Fig. 8). The spectral area at each temperature (A_T) is scaled by the mean value of the spectral area obtained at RT ($\langle A_{RT}\rangle$). The area A_T can be calculated as follows (A_{RT} is calculated using the same expression):

$$A_T = \frac{A_L}{B\,\lambda} \sum_i^n C_i \Gamma_i , \tag{3}$$

where n stands for the number of sites present in the spectrum, A_L is the total Lorentzian amplitude (the thin source approximation is valid due to the reasons discussed in previous section), B denotes the baseline (number of counts far-off resonance), C_i stands for the ith site contribution, Γ_i represents the linewidth corresponding to C_i, and λ is defined in data collection subsection.

One can define effective mean-squared displacement (MSD) relative to the effective RT MSD as $-1/k^2 \ln(A_T/\langle A_{RT}\rangle)$. The evolution of the above MSD versus temperature T has been approximated by the following relationship:

$$-\frac{1}{k^2}\ln\left(\frac{A_T}{\langle A_{RT}\rangle}\right) = C + (\alpha\, T + \beta)\,\frac{e^x}{1+e^x} \tag{4}$$

with k denoting the wave number of the 14.4-keV Mössbauer radiation (7.3 Å^{-1}) and x taking on the form

$$x = \frac{T - T_0}{Q}. \tag{5}$$

Parameters C, α, β, T_0, and Q were fitted to the data yielding curve shown in Fig. 8. The characteristic temperature $T_0 = 640(33)$ K.

In the temperature range between 800 and 1200 K the function described by the relation (4) is linear versus T in accordance with the Debye model. The onset of channel diffusion can be observed and accounts for the considerable increase in MSD, e.g., the characteristic drop in the spectral area. One has to note, that while the temperature is raised the significant part of ^{57}Co residing in lattice positions at RT can transfer into the channel and become a fast diffuser. Hence such process results in additional increase of the MSD. Therefore the shape of the MSD function versus temperature indicates that the energy of the interstitial Co/Fe is higher than the energy of the substitutional Co/Fe. The data below 500 K belong to the quantum region, where the recoilless fraction is almost temperature independent. It should be mentioned that they could not be reliably evaluated due to the quite significant statistical errors. The values and their

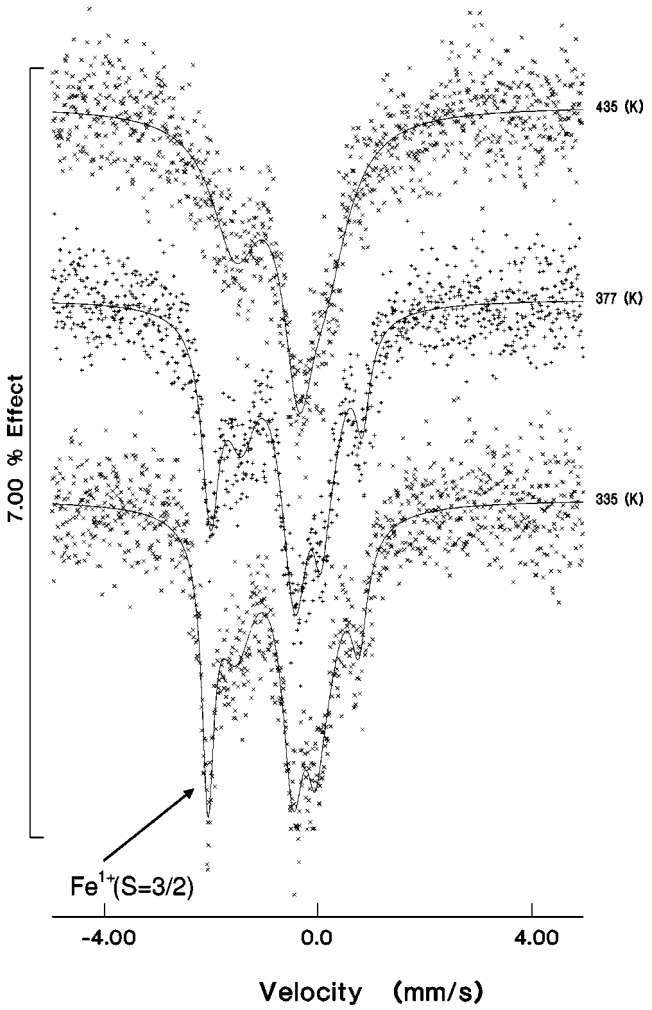

FIG. 7. Mössbauer spectra versus temperature of the annealed and quenched sample showing disappearance of the channel components due to the very fast diffusivity. Sample oriented at ⟨111⟩ direction.

standard deviations are of the same order. Thus negative values for MSD at low temperatures have no physical meaning.

A gradual ''conversion'' of Fe^{2+} ($S=2$) into Fe^{2+} ($S=0$) at perturbed lattice sites could be explained by invoking defect (oxygen vacancy) mobility with the increasing temperature. A lattice thermal expansion makes the crystal apparently more covalent, and hence Fe^{3+} isomer shift moves gradually towards Fe^{2+} shift, i.e., an apparent reduction occurs (see Fig. 6).

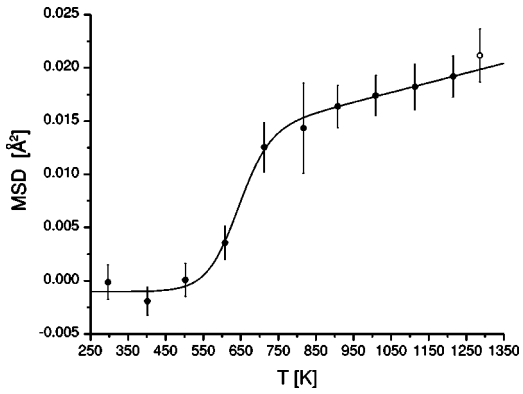

FIG. 8. Effective MSD versus temperature. The highest temperature point (open circle) was excluded from the fitting procedure due to the onset of anharmonicity.

A quadrupole interaction experienced by Fe^{2+} ($S=2$) diminishes with the increasing temperature due to the thermal equilibration of the crystal field levels. The substitutional iron diffuses slowly even at high temperatures as one cannot see any line broadening. This finding is in agreement with the tracer results of Sasaki *et al.*[5] and indicates that the jump barrier from the channel to the lattice positions is high. The parameter MSD becomes nonlinear as a function of T at highest temperatures (see Fig. 8) due to the onset of the vibrational lattice anharmonicity.

ACKNOWLEDGMENTS

Professor Georges Dénès from Department of Chemistry and Biochemistry, Concordia University, Montreal, Quebec, Canada and Dr. Francine Bélanger-Gariépy from Département de Chimie, Université de Montréal, Montréal, Québec, Canada are thanked for their invaluable help with x-ray-diffraction experiments on rutile crystals. Dr. Bogdan Sepioł from Institut für Materialphysik der Universität Wien, Austria is acknowledged for his aid in rocking curve measurements. This work was financed by KBN (National Committee for Scientific Research, Poland) under Grant No. 2 P302 193 05.

*Email address: sfwdowik@cyf-kr.edu.pl

[1] F. Millot, M. G. Blanchin, R. Tétot, J. F. Marucco, B. Poumelles, C. Picard, and B. Touzelin, Prog. Solid State Chem. **17**, 263 (1987).
[2] L. A. Dominik and R. K. MacCorne, Phys. Rev. **156**, 910 (1967).
[3] L. A. Dominik and R. K. MacCorne, Phys. Rev. **163**, 756 (1967).
[4] R. N. Blumenthal, J. Baukus, and W. M. Hirthe, J. Electrochem. Soc. **114**, 172 (1967).
[5] J. Sasaki, N. L. Peterson, and H. Hoshino, J. Phys. Chem. Solids **46**, 1267 (1985).
[6] K. Hoshino, N. L. Peterson, and C. L. Wiley, J. Phys. Chem. Solids **46**, 1397 (1985).
[7] P. P. Stampfl, J. C. Travis, and M. J. Bielefeld, Phys. Status Solidi A **15**, 181 (1973).
[8] T. R. Sandin, D. Schroeer, and C. D. Spencer, Phys. Rev. B **13**, 4784 (1976).
[9] G. Vogl, Hyperfine Interact. **53**, 197 (1990).
[10] M. Kwater, M. Pochroń, K. Ruebenbauer, T. Terlecki, U. D. Wdowik, and R. Górnicki, Acta Phys. Slov. **45**, 45 (1995).
[11] J. G. Mullen, A. Djedid, G. Schupp, D. Cowan, Y. Cao, M. L. Crow, and W. B. Yelon, Phys. Rev. B **37**, 3226 (1988).
[12] S. L. Ruby, Mössbauer Effect Methodology **8**, 263 (1979).
[13] K. Ruebenbauer, Report No. 1133/PS Institute of Nuclear Physics, Cracow, 1981.
[14] M. de Coster and S. Amelinckx, Phys. Lett. **1**, 254 (1962).
[15] J. G. Mullen, Phys. Rev. **131**, 1415 (1963).

[16] J. Chappert, R. B. Frankel, and N. A. Blum, Phys. Lett. **25A**, 149 (1967).
[17] R. B. Frankel and N. A. Blum, Bull. Am. Phys. Soc. **12**, 24 (1967).
[18] J. Chappert, R. B. Frankel, and N. A. Blum, Bull. Am. Phys. Soc. **12**, 352 (1967).
[19] D. L. Nagy (private communication).